CHAPTER 3

STRUCTURAL SURVEY OF THE PEROXIREDOXINS

P. ANDREW KARPLUS AND ANDREA HALL
Department of Biochemistry and Biophysics, Oregon State University, Corvallis, OR 97331

Abstract: Peroxiredoxins (Prxs) are ubiquitous proteins that use an active site Cys residue to reduce hydroperoxides. Structural studies since the first Prx structure was determined in 1998 have produced 35 crystal structures of wild type and mutant Prxs with at least one representative structure from each of the five major evolutionary subfamilies of Prxs. These structures have yielded a great deal of knowledge about Prx structure and structure-function relations, revealing fascinating variations in quaternary structure and details of the fully-folded and locally-unfolded conformations that are involved in the catalytic cycle of all Prxs

Keywords: Protein structure, Peroxiredoxin families, Local unfolding, Conformational change, Active site

1. SCOPE AND PURPOSE

A protein's function flows directly from its structure, and for this reason knowledge of the three-dimensional structures of proteins plays a crucial role in guiding our understanding of protein function at the molecular level. In this regard, structure encompasses not only a set of coordinates, but also the dynamic and energetic properties of a protein. Since this chapter on peroxiredoxin (Prx) structure is present in the context of a whole volume documenting biochemical, enzymatic, physiological and regulatory aspects of Prxs, this review will not be a full synthesis of structure-function relations of Prxs, as was recently provided by Wood *et al.* (2003b), but will highlight and synthesize the key aspects of what is known today about the Prx structures themselves. It is designed so that when read together with Chapters **2, 4** and **5**, it will give a complete picture of Prx structure-function relations. Also, whereas all of the currently known Prx structures will be cataloged here, it is not possible in this review to capture all of the ideas and insights that are present in the reports that describe these Prx structures in the original literature, so readers are encouraged to dig into the original structure reports (see citations in Table 1) in order to benefit from the descriptions and insights they have to offer.

L. Flohé and J. R. Harris (eds.), Peroxiredoxin Systems, 41–60.

Table 1. Deposited crystal structures of Prxs[a]

	Structure	Oligomer state	Interface type	Redox[b] State	Conformation[c]	Mutation	PDB code	Resolution (Å)	Reference
Prx1									
1	*Hs*PrxII	$(\alpha_2)_5$	BA	51SO_2H172	FF	–	1QMV	1.7	(Schröder *et al.*, 2000)
2	*Rn*PrxI	α_2	B[d](A)	52SS173	$LU_{PRX1''}$	C83S	1QQ2	2.6	(Hirotsu *et al.*, 1999)
3	*Bt*PrxIII	$(\alpha_2)_6$[e]	BA	47SH168	FF	C168S	1ZYE	3.3	(Cao *et al.*, 2005)
4	*Tc*TXNPx	$(\alpha_2)_5$	BA	52SH173	FF	–	1UUL	2.8	(Pineyro *et al.*, 2005)
5	*Cf*TryP	$(\alpha_2)_5$	BA	52SH173	LU_{PRX1}	–	1E2Y	3.2	(Alphey *et al.*, 2000)
6	*Hp*AhpC	$(\alpha_2)_5$	BA	49SS169	LU_{PRX1}	–	1ZOF	2.95	(Papinutto *et al.*, 2005)
7	*Pv*2Cys	$(\alpha_2)_5$	BA	50SS170	LU_{PRX1}	–	2H66	2.5	Unpublished
8	*Py*PrxI	$(\alpha_2)_4$	BA	44SH164	LU_{PRX1}	–	2H01	2.3	Unpublished
9	*Mt*AhpC	$(\alpha_2)_6$	BA	61SS174	$LU_{PRX1'}$	C176S	2BMX	2.4	(Guimaraes *et al.*, 2005)
10	*St*AhpC	$(\alpha_2)_5$	BA	46SS165	LU_{PRX1}	–	1YEP	2.5	(Wood *et al.*, 2002)
11	*St*AhpC	$(\alpha_2)_5$	BA	46SS165	LU_{PRX1}	T77D	1YEX	2.3	(Parsonage *et al.*, 2005)
12	*St*AhpC	$(\alpha_2)_5$	BA	46SS165	LU_{PRX1}	T77I	1YF0	2.5	(Parsonage *et al.*, 2005)
13	*St*AhpC	$(\alpha_2)_5$	BA	46SS165	LU_{PRX1}	T77V	1YF1	2.6	(Parsonage *et al.*, 2005)
14	*St*AhpC	$(\alpha_2)_5$	BA	46SH[f]165	FF	C46S	1N8J	2.17	(Wood *et al.*, 2003)
15	*Ax*AhpC	$(\alpha_2)_5$	BA	47SS166	LU_{PRX1}	–	1WE0	2.9	(Alphey *et al.*, 2000)
Prx6									
16	*Hs*PrxVI	α_2	B	47SOH	FF	C91S	1PRX	2.0	(Choi *et al.*, 1998)
17	*Py*1Cys	α_2	B	47SH	FF	–	1XCC	2.3	Unpublished
18	*Ap*Tpx	$(\alpha_2)_5$	BA	50SO_3H213	FF	–	2CV4	2.3	(Mizohata *et al.*, 2005)
19	*Ap*Tpx	$(\alpha_2)_5$	BA	50SH213	FF	C207S	1X0R	2.0	(Nakamura *et al.*, 2006)
Prx5									
20	*Hs*PrxV	α_2	A	47SH151	FF	–	1H4O	1.95	Unpublished
21	*Hs*PrxV	α_2[g]	A	47SH151	FF	–	1HD2	1.5	(Declercq *et al.*, 2001)
22	*Hs*PrxV	α_2	A	47SS151	LU_{PRX5}	–	1OC3	2.0	(Evrard *et al.*, 2004)
23	*Hs*PrxV	α_2	A	47SH[f]151	FF	C47S	1URM	1.7	(Evrard *et al.*, 2004)
24	*Pt*PrxD	α_2	A	51SH	FF	–	1TP9	1.62	(Echalier *et al.*, 2005)
25	*Hi*HyPrxV	α_2[h]	A	49SH	LU_{PRX5}	–	1NM3	2.8	(Kim *et al.*, 2003)
26	*Pf*AOP	α_2	A	59SO_3H	FF	–	1XIY	1.8	(Sarma *et al.*, 2005)

Tpx									
27	*Ec*Tpx1	α_2	A	61SS95	LU_{TPX}	–	1QXH	2.2	(Choi *et al*., 2003)
28	*Hi*Tpx	α_2	A	59SS93	LU_{TPX}	–	1Q98	1.9	Unpublished
29	*Mt*Tpx	α_2	A	60SH[f]93	FF	C60S	1Y25	2.1	(Stehr *et al*., 2006)
30	*Sp*Tpx	α_2	A	58SH92	FF	–	1PSQ	2.3	Unpublished
BCP									
31	*Ap*BCP	α_2	A	49SH/SS54	FF/LU_{BCP}	–	2CX4	2.3	Unpublished
32	*Ap*BCP	α_2	A	49SS54	LU_{BCP}	–	2CX3	2.6	Unpublished
33	*Sc*nTPx	α	–	107SH[f]112	FF	C107S/C112S	2A4V	1.8	(Choi *et al*., 2005)
???[i]									
34	*Mt*AhpE	α_2[j]	A	45SH	FF	–	1XXU	1.9	(Li *et al*., 2005)
35	*Mt*AhpE	α_2[j]	A	45SOH	FF	–	1XVW	1.87	(Li *et al*., 2005)

[a] Organism abbreviations are as follows:
Ap=Aeropyrum pernix; *Ax=Amphibacillus xylanus*; *Bt=Bos taurus*; *Cf=Crithidia fasciculata*; *Ec=Escherichia coli*; *Hi=Haemophilus influenzae*; *Hp=Helicobacter pylori*; *Hs=Homo sapiens*; *Mt=Mycobacterium tuberculosis*; *Pf=Plasmodium falciparum*; *Pt=Populus trichocarpa*; *Pv=Plasmodium vivax*; *Py=Plasmodium yoelii*; *Rn=Rattus norvegicus*; *Sc=Saccharomyces cerevisiae*; *Sp=Streptococcus pneumoniae*; *St=Salmonella typhimurium*; *Tc=Trypanosoma cruzi*

[b] The redox state of C_P is given as well as the residue numbers of C_P and, for 2-Cys Prxs, C_R.

[c] The conformation of the active site is indicated as FF for fully-folded and LU with subscripts for the kinds of local unfolding seen in various subfamilies (see Figure 5).

[d] This disulfide form shows only the stable B-type dimer, but the protein is believed to be a BA decamer in the reduced state.

[e] A concatameric interaction of the dodecamers is believed to be an artifact of crystallization.

[f] A Cys → Ser mutant of C_P mimics the reduced state.

[g] Originally described as a monomer when published by the authors but later acknowledged as A-type dimer (Evrard *et al*., 2004).

[h] The glutaredoxin domains interact to make the protein a dimer of dimers.

[i] *Mt*AhpE does not clearly fit into any of the designated subfamilies and so has been set apart.

[j] The authors described the structures as an $(\alpha_2)_4$ octamer, but we suspect (see text) the octamer is an artifact of high protein concentration. Also, the FF form in entry 1XXU is as seen for other subfamilies, but that in 1XVW is slightly different.

2. INTRODUCTION

As first recognized in 1994 (Chae *et al*., 1994) Prxs are a widely distributed family of peroxide reducing enzymes that evidence suggests have evolved from an ancestor protein having the thioredoxin fold (Copley *et al*., 2004). All of the known Prx sequences share recognizable similarities, including an absolutely conserved Cys residue (called the peroxidatic Cys) that is involved directly in the reduction of the substrate hydroperoxides. As outlined in Chapter 2, the known Prx sequences can be organized into five major subfamilies, each constituting a group of proteins that are more similar to each other than to the other Prxs. This grouping based on sequence similarity is most useful here because the level of structural similarity observed between two homologous proteins is generally related to their level of sequence similarity (Chothia and Lesk,1986). For the sake of consistency, we will here use the nomenclature introduced in Chapter 2, with the five subfamilies being referred to as Prx1, Prx6, Prx5, Tpx and BCP (shortened from BCP/PrxQ). In terms of the Prxs from humans, subfamily Prx1 contains human PrxI, II, III and IV, subfamily Prx6 contains PrxVI, and subfamily Prx5 contains PrxV. Subfamily Tpx contains only bacterial Prxs and subfamily BCP contains bacterial and plant (PrxQ) Prxs. Subfamilies Prx1 and Prx6 are listed next to each other as they are similar enough to each other that in some reports they are grouped into a single subfamily (e.g. Copley *et al*., 2004).

It is wise to be cautious about assigning a particular Prx to a subfamily just based on the common name of the enzyme, because many individual Prxs were named based on their activities before it was known which ones were most similar to each other. For example, within the Prx1 subfamily individual enzymes have a variety of common names ranging as widely as PrxI, PrxII, PrxIII, PrxIV, Tsa1, PrxA, PrxB, Tpx1, and AhpC. In terms of labels based on mechanism, all "typical 2-cys" Prxs are in the Prx1 and Prx6 subfamilies, while "atypical 2-Cys Prxs", and "1-Cys Prxs" are not associated with any family in particular, but are distributed among a variety of families (see section 6.2 below).

3. UNIVERSAL FEATURES OF THE PRX CATALYTIC CYCLE

A combination of structural and enzymatic studies has revealed that all Prxs have in common a catalytic cycle that includes a crucial conformational step as well as (at least) three chemical steps (Figure 1). Throughout this Chapter, the Cys that directly reduces peroxide will be referred to as the peroxidatic Cys, using S_P to designate the sulfur atom of the Cys side chain and using C_P to designate the residue. Similarly, the resolving thiol, the thiol that forms a disulfide with C_P, will be designated by S_R for the sulfur atom and C_R for the residue if it is a Cys.

As seen in Figure 1, the catalytic cycle begins with the peroxide substrate (either an alkyl hydroperoxide or hydrogen peroxide) entering the fully-folded substrate binding pocket and reacting with the peroxidatic Cys (C_P) at the base of this pocket. In chemical step 1, the peroxide substrate is reduced to its corresponding alcohol and

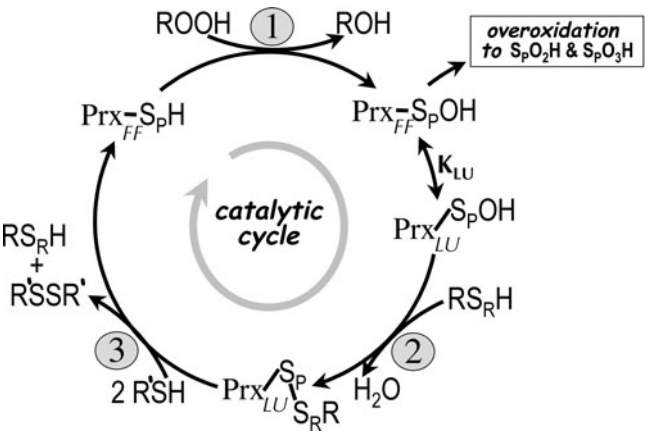

Figure 1. The universal catalytic cycle of Prxs. The three main chemical steps of (1) peroxidation, (2) resolution, and (3) recycling are shown along with an explicit local unfolding step required for the resolution reaction. S_P and S_R designate the sulfur atoms of the peroxidatic and resolving thiols, respectively. The fully-folded and locally-unfolded enzyme conformations are designated as FF and LU, respectively. See the text for further details

C_P becomes oxidized to the sulfenic acid form (S_POH). Resolution (step 2) occurs when a free thiol (S_RH) attacks the S_POH to release water and form a disulfide. This attacking thiol, whether present on the same or another subunit ot the Prx, is referred to as the resolving thiol, as it resolves a potential block of the catalytic cycle resulting from the poor accessibility of C_P by the bulky natural substrate. Because in the fully-folded enzyme C_P is located in a protected active site pocket, resolution cannot occur without a conformational change that involves (at a minimum) the local unfolding of the active site pocket so as to make the C_P side chain much more accessible. It is expected that the locally-unfolded and fully-folded conformations of the protein are in a dynamic equilibrium, governed by the equilibrium constant K_{LU} that may differ for different Prxs and for the various redox states of each Prx. Because disulfide formation involves the adduction to C_P of a large group, the disulfide forms of Prxs cannot adopt the fully-folded conformation, but remain locked into a locally-unfolded conformation. The reaction cycle is completed when the disulfide form is recycled to regenerate the peroxidatic and resolving thiols (step 3), and the Prx is freed to again adopt the fully-folded peroxidatic active site. In principle, recycling may involve protein or small molecule thiols. For many Prxs this step is known to involve a thioredoxin-like dithiol containing protein or domain (see Chapter **4**).

While it is not part of the normal productive catalytic cycle, in competition with the resolution reaction is an overoxidation reaction (Figure 1). In this side reaction, the fully-folded S_POH form reacts with a second molecule of peroxide to form a sulfinic acid (S_PO_2H) and in certain Prxs this can further react with a third peroxide substrate to yield a terminally oxidized sulfonic acid (S_PO_3H) form.

As discussed by Sarma *et al*. (2005), the terminal state for a given Prx appears to be governed by details of the active site geometry. In any case, neither of these "overoxidized" forms can be readily converted to a disulfide and thus represent inactive forms of the enzyme, although the S_PO_2H form of certain eukaryotic Prxs is thought to be physiologically relevant in peroxide signal transduction (Wood *et al*., 2003; Immenschuh *et al*., 2005; Kang *et al*., 2005; Chapters **14 & 15**) and can be resurrected to S_POH in an ATP dependent reaction (Biteau *et al*., 2003; Woo *et al*., 2003; Chang *et al*., 2004). The structural studies summarized in the next section reveal not only representative fully-folded and locally unfolded structures for various Prx subfamilies, but also interesting variations in quaternary structure that add complexity to the structure-function relations.

4. SUMMARY OF STRUCTURAL INVESTIGATIONS

Since the first Prx crystal structure was reported in 1998 (Choi *et al*., 1998), the field has rapidly matured so that as of July 2006, as summarized in Table 1, 35 crystal structures of Prxs are available in the Protein Data Bank (Berman *et al*., 2000). Although three Prxs from the Prx5 subfamily have been analyzed by NMR to the point of making resonance assignments (Trivelli *et al*., 2003; Bouillac *et al*., 2004; Echalier *et al*., 2005), no complete NMR-derived structures are in the protein Data Bank. The 35 available structures represent the wild type and/or mutant forms of 25 distinct Prxs, including at least one representative from each Prx subfamily: eleven from subfamily Prx1, three from subfamily Prx6, four from subfamily Prx5, five from subfamily Tpx, and two from subfamily BCP. Eight of the structures, some of which are derived from structural genomics projects, have not yet been described in a publication in the original literature. In terms of the redox state of the peroxidatic Cys residue, all possibilities have been seen from SH, SOH, SO_2H, SO_3H and SS, although in only three cases, those of AhpC from *Salmonella typhimurium* (subfamily Prx1), human PrxV (subfamily Prx1), and a BCP from *Aeropyrum pernix* have both SH and SS states been observed for the same protein.

5. STRUCTURAL FEATURES COMMON TO ALL PRXS

5.1. Overall Structure

At the topology level, all Prxs have core tertiary structures that are highly spatially conserved (Figure 2a) with variations in loop lengths and conformations and N- and C-terminal extensions. When schematized, the core structure can be seen to include 7 β-strands and 5 α-helices, which are organized as a central 5-stranded antiparallel β-sheet, including strands β5–β4–β3–β6–β7, with one face of the sheet covered by β1–β2–α1 and α4 and the other face of the sheet covered by α2, α3 and α5 (Figure 2b). Because strand β5 has some interaction with strand β1, the central sheet is sometimes referred to as a single 7-stranded sheet rather than a 5-stranded

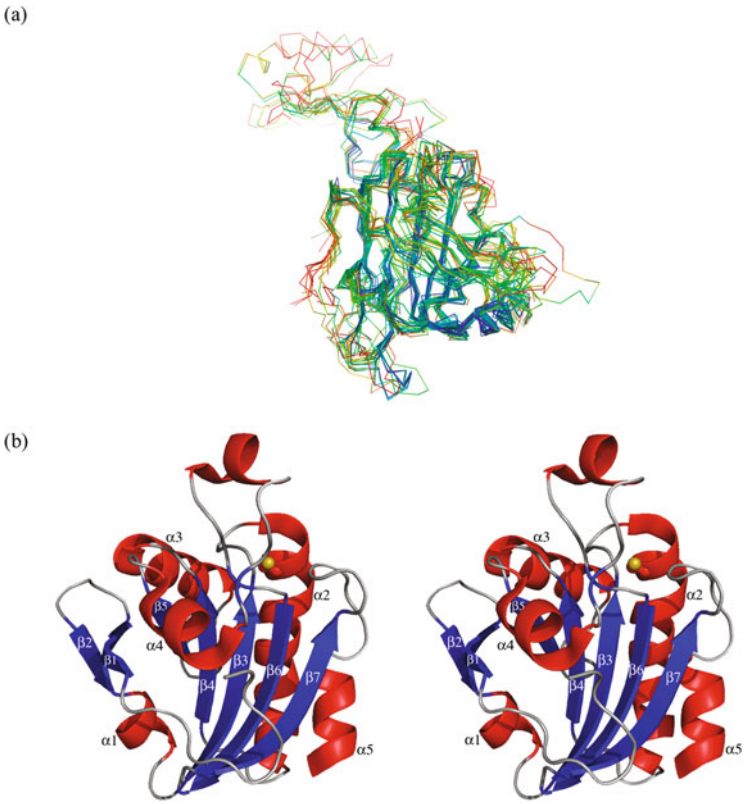

Figure 2. The Prx fold. (a) An overlay of all 19 fully-folded Prx structures indicating the conservation of the core of the fold. Colored by mobility with deep blue representing the least mobile portions of the chain and bright red representing the most mobile portions. (b) Stereoview of a representative fully-folded Prx (PDB code 1HD2) labeled to identify the common core α-helices (red), and β-strands (blue) that are conserved among all Prx proteins. The peroxidatic cysteine in the first turn of helix α2 is shown as a ball and stick with S_P in mustard yellow (See Plate 1)

sheet plus an additional 2-stranded β–hairpin. In the fully-folded conformation of Prxs (as shown in Figure 2) the C_P-residue is always located in the first turn of helix α2, and the unraveling of the first turn or two of this helix appears to be a universal feature of local unfolding.

In crystal structures, in addition to the coordinates, temperature factors (or B-factors) are derived for each atom. These values give information about the level of mobility of the structure, with larger values implying more disordered regions. In Figure 2a, the coloring of the Prx structure indicates the level of order, with a color gradient extending from the less mobile portions being blue to the most mobile portions being red. Figure 2a makes it very clear that surface loops are in general the most mobile parts of the structure, and these are also the regions that vary most in conformation and in the presence of insertions and deletions.

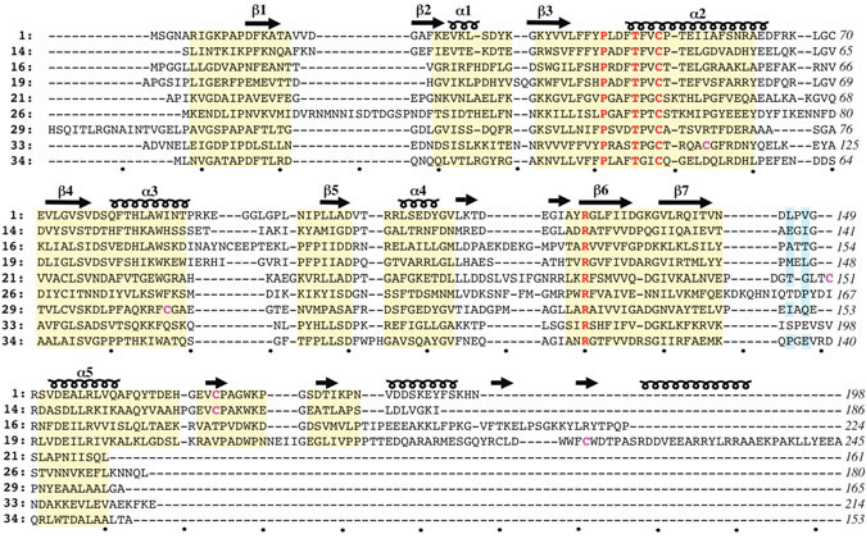

Figure 3. Structure based sequence alignment of representative Prxs. Regions of common main-chain path are highlighted by a tan background. Secondary structure elements are indicated by coils (α-helices, 3_{10}-helices) and arrows (β-strands) above the sequence, and core elements are labeled as in figure 2b. Four residues absolutely conserved are colored red and C_R of 2-Cys Prxs are colored violet. Residues involved in passing chain stabilization of the active site Arg are highlighted by a cyan background. Structures are referenced by index number from Table 1 and include in order a sensitive Prx1, a robust Prx1, a 1-Cys Prx6, a 2-Cys Prx6, a 2-Cys Prx5, a 1-Cys Prx5, a Tpx, a BCP, and the difficult to classify *Mt*AhpE. Reference residue numbers are at the end of each line and for convenience, dots below the sequence blocks mark every ten spaces. Structure based sequence alignment was aided by the use of Sequoia (Bruns *et al*., 1999) (See Plate 2)

Figure 3 presents a structure-based sequence alignment that includes representative Prxs from each of the five subfamilies. This alignment reveals in a different way how insertions and deletions in the various families are generally located between the common core secondary structural elements.

5.2. The Fully-folded Peroxidatic Active Site

As was noted above, in the fully-folded enzyme the peroxidatic active site is located in a pocket with the C_P residue present in the first turn of helix α2. A comparison of the active sites of all of the fully-folded structures (Figure 4a) shows that the geometry of this region is highly conserved despite the broad sequence diversity represented among the five subfamilies. In addition to the peroxidatic Cys, there are a Pro, a Thr and an Arg that are absolutely conserved in known Prx sequences (Figure 3). These three residues are all located directly in the fully-folded peroxidatic active site and are in van der Waals contact with C_P (Figure 4b). The high structural conservation of the active site among Prxs means that one structure can be used to represent the

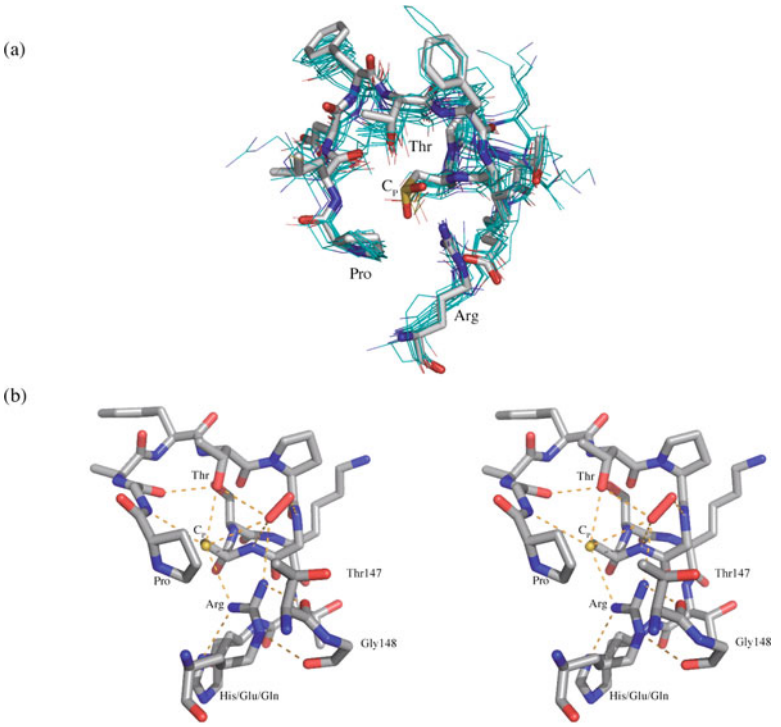

Figure 4. The peroxidatic active site of Prxs. (a) An overlay of fully-folded Prx structures (thin lines with atom coloring C=cyan, N=blue, O=red, S=mustard) to indicate the high conservation of the peroxidatic active site geometry. Included are residues in the segment surrounding C_P and the conserved Arg. PDB entry 1QMV is modeled as sticks with atom coloring (C=grey, N=blue, O=red, S=yellow). (b) Stereoview of the fully-folded active site of human PrxV (Declercq *et al*., 2001), the highest resolution structure (PDB code 1HD2). This active site has a bound molecule of benzoate, and in this figure, we have inserted a peroxide molecule close to the positions occupied by the benzoate oxygens (see text). Potential H-bonding interactions (dashed lines) are shown. In addition to the residues shown in (a), two residues (Thr147 and Gly148) from the loop between strand β7 and helix α5 are also included as they stabilize the Arg by their peptide oxygens. In Figure 3, the residues contributing equivalent carbonyls are highlighted with a cyan background. Although not seen in the BCP structure selected for Figure 3, the other BCP structure (PDB entry 2CX4) does conserve this feature (See Plate 3)

interactions common to all. Fortuitously, the highest resolution image of the fully-folded active site as seen in human PrxV (Declercq *et al*., 2001), has a bound molecule of benzoate, which we speculate binds as a substrate analog with the two carboxylate oxygens crudely mimicking the placement of the two oxygens of a peroxide substrate.

The interactions of various residues can be seen in Figure 4b. The conserved Arg is positioned by three H-bonds (one to a His conserved as His or Glu in most Prxs and two to peptide oxygens from the loop between strand β7 and helix α5), while the other two H-bonds of the Arg point at S_P and the peroxide oxygen to be attacked. A second H-bond to S_P comes from the backbone amide located just after

the conserved Pro. The Thr residue has an interesting position where it approaches closely to both a benzoate oxygen and the backbone oxygen of the residue following the conserved Pro. Both of these atoms are H-bond acceptors so one of these close approaches is expected to be an unfavorable electrostatic repulsion, because normally Thr can only donate one H-bond. Two final important interactions are H-bonds from two peptide nitrogens in the first turn of helix α2 to the benzoate oxygens.

The interactions seen support the idea that the benzoate is mimicking peroxide, although inaccurately, since the peroxide bond length is 1.4 Å while the O···O separation in benzoate is ∼2.3 Å. The closer O···O separation in peroxide would allow it to make much better H-bonds to the two backbone amides. In terms of proposed roles for the three conserved residues, the Pro shields the C_P from water and positions the peptide NH that contributes to C_P activation, the Arg not only activates C_P, but also influences the position and chemistry of the peroxide oxygen that will be attacked, and the Thr may play a role as a proton shuttle possibly between C_P and/or the two oxygens of the peroxide. In addition, the peptide amide from C_P and the residue preceding it play crucial roles in positioning the two oxygens of the peroxide, and stabilizing them as they separate during catalysis.

5.3. Local Unfolding of the Peroxidatic Active Site

Currently, structures are available for locally-unfolded disulfide bonded forms of four of the five Prx subfamilies; the one missing is subfamily Prx6. Although there are variations in the details of the local unfolding transition(s) of each subfamily, they all have in common an unraveling of the first turn of helix α2 so that C_P itself is no longer in a helix but is highly exposed in a loop segment (Figure 5). In

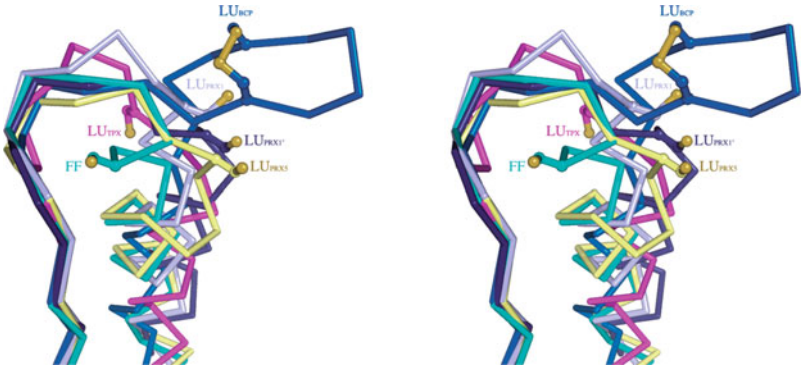

Figure 5. Local unfolding transitions of the peroxidatic active site region. Stereoview comparing the structure of the canonically fully-folded helix α2 (cyan for PDB entry 1QMV) compared with a set of representative locally-unfolded C_P loops: two from subfamily Prx1 (light purple for PDB entry 1YEX and dark purple for PDB entry 2BMX), and one each from subfamilies Prx5 (yellow for PDB entry 1OC3), Tpx (magenta for PDB entry 1QXH) and BCP (dark blue for PDB entry 2CX3). The C_P residue is in each case shown as ball and stick with S_P in mustard yellow. The LU structures are all involved in disulfide bonds even though the C_R is only shown for the LU_{BCP} case (See Plate 4)

Prx structure descriptions, this loop is sometimes referred to as the C_P-loop (Wood *et al*., 2002). Further aspects of the locally unfolded structures are unique to each subfamily, and so will be presented in the sections below.

6. FEATURES VARYING BETWEEN PRX SUBFAMILIES

6.1. Quaternary Structures

The peroxidative active site only includes residues from a single monomer, so in principle Prxs could be monomeric. Among structurally known Prxs, however, only one, the BCP from *Saccharomyces cerevisiae*, appears to be monomeric (entry #33, Table 1). The remaining ones have quaternary structures that include two distinct kinds of dimers, as well as octamers, decamers and dodecamers (Figure 6). To fit into this categorization, three Prxs require some additional explanation. First is the hybrid Grx-Prx from *Haemophilus influenza* (entry #25 in Table 1) which is actually tetrameric. We treat it here as dimeric because structurally it is made up of two dimeric Prxs that are joined to make a tetramer by dimerization interactions of the Grx domains of the protein (Kim *et al*., 2003). Thus as far as the Prx interactions, it is dimeric. Second is *Mycobacterium tuberculosis* AhpE (entries #34 and #35 in Table 1) which was reported to be an octamer (Li *et al*., 2005), but two reasons lead us to suspect that the octamer is an artifact of crystallization rather than a physiologically relevant state: Most importantly, gel filtration at high concentration showed the large majority of the protein was present as a dimer with only a little octamer present, and less conclusive but still of interest to note, the interface building the octamers was not very extensive and did not involve the known B-type interface (see section 6.1.1 below). The third structure requiring comment is the structure of *Bos taurus* PrxIII (entry #3 in Table 1) which in the crystal was seen to be a remarkable concatenated pair of dodecamers (Cao *et al*., 2005). The authors opined that the concatenation was an artifact, and that the physiological state of the protein is a single dodecamer as was seen for *M. tuberculosis* AhpC (entry #9 in Table 1; Guimaraes *et al*., 2005).

6.1.1. A-type and B-type interfaces

All oligomeric Prxs are formed via associations involving only two distinct interfaces. One of these interfaces, as seen in Figure 6b, involves the edge to edge association of strands β7 of the central β-sheet of two Prx chains to make an extended 10-stranded β-sheet (or a 14-stranded sheet if one considers the monomer topology to be a 7-stranded sheet). The other interface is a tip-to-tip association centered on helix α3 packing against its counterpart in the other chain. Following the suggestion of Sarma *et al*. (2005), we refer to these interfaces as the B-type interface (B for "β-sheet" based) and the A-type interface (A for "alternate" or for "ancestral"), respectively. Prxs with B-type interfaces have in common a C-terminal subdomain that reaches out across the two-fold axis to make extensive interactions that help stabilize the dimer. For more detailed descriptions of the A and B-type interfaces readers are referred to treatments in the original literature (Choi *et al*.,

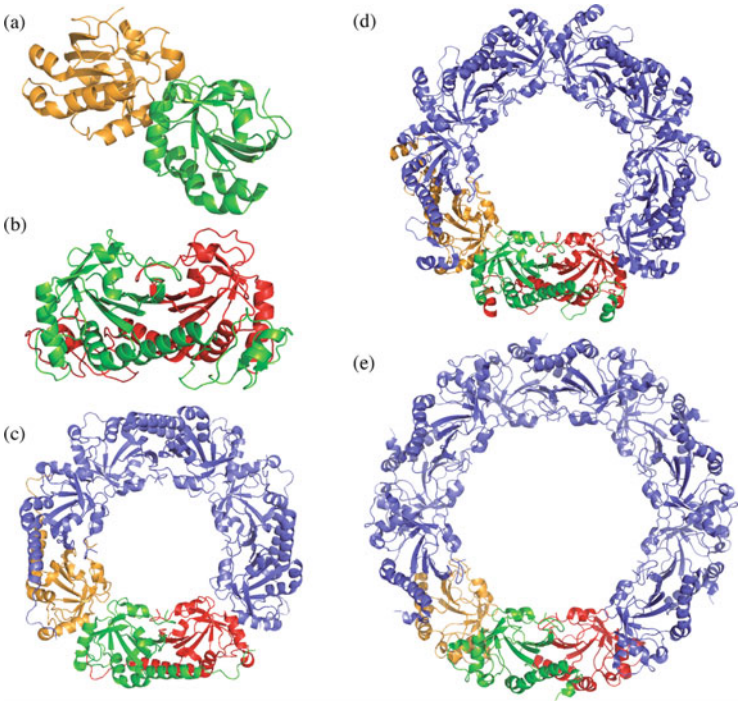

Figure 6. Quaternary structures of Prxs. Shown are representative structures of an (a) A-type dimer (PDB entry 1HD2), (b) B-type dimer (PDB entry 1PRX), (c) octamer (PDB entry 2H01), (d) decamer (PDB entry 1QMV) and (e) dodecamer (PDB entry 2BMX). Subunit coloring for the A-type dimer (gold and green) and the B-type dimer (green and red) are used in the higher order structures to show how they are built from these two types of interactions. The octamer, decamer and dodecamer are on the same scale and have inner diameters of ~50 Å, ~60 Å and ~70 Å, respectively (See Plate 5)

1998; Wood *et al*., 2002; Choi *et al*., 2003; Echalier *et al*., 2005; Sarma *et al*., 2005).

As seen in Table 1, both subfamilies Prx1 and Prx6 have dimeric Prxs with the B-type interface (Figure 6b), but subfamilies Prx5 and Tpx exist exclusively as A-type dimers (Figure 6a). One BCP subfamily structure appears to be monomeric (having no packing interactions in the crystal involving either the A- or B-type interface), but the other BCP representative has tight packing interactions in the crystals that involve the A-type interface, so we have tentatively identified it as an A-type dimer (Table 1). The relative orientation of subunits interacting via the A-type interface may differ by up to ~30° among various Prxs (Sarma *et al*., 2005). In terms of higher order oligomers, the octameric, decameric and dodecameric Prxs are exclusive to the Prx1 and Prx6 subfamilies and consist of four, five or six B-type dimers associating to form the higher order structure via A-type interfaces (Figure 6c,d,e). Comparisons reveal that the tighter ring structure of the octamer and the expanded ring structure of the dodecamer are due to shifts in the packing at

the B-type interface with the A-type interfaces being equivalent. We expect based on this that octameric, decameric, and dodecameric Prxs will function equivalently despite the difference in appearance; for simplicity, in the remainder of this review, any properties of decameric Prxs that are discussed are expected to refer equally well to octamers and dodecamers.

6.1.2. A linkage of decamer assembly and the catalytic cycle

As first shown by Wood *et al*. (2002) and since confirmed by Guimaraes *et al*. (2005), decameric Prxs have a redox-linked quaternary structure, with disulfide formation weakening decamer stability so that the disulfide form of the enzyme is present as B-type dimers (or mixtures of dimers and higher order oligomers) and all other forms of the enzyme (S_PH, S_POH, S_PO_2H, S_PO_3H) expected to be present as stable decamers. The dimer-decamer equilibrium is also influenced somewhat by pH and ionic strength (Schröder *et al*., 1998; Kitano *et al*., 1999; Kristensen *et al*., 1999; Schröder *et al*., 2000; Chauhan and Mande, 2001; Papinutto *et al*., 2005), but these factors are not expected to vary much *in vivo*. The proposed physical explanation for the linkage between disulfide formation and decamer disruption is that the fully-folded active site butresses the decamer building (A-type) interface and when the local-unfolding of the active site is locked into place by disulfide formation, the decamer is destabilized (Wood *et al*., 2002). Thus, during the catalytic cycle (Figure 1) these enzymes undergo a change from decamers to dimers and back to decamers again (Wood *et al*., 2002). If correct, this explanation implies that for decameric Prxs enzymes, the stability of the fully-folded active site conformation (and hence catalytic activity) is linked to decamerization. This link was confirmed by a study showing that mutants of *S. typhimurium* AhpC that could not effectively form decamers were 100-fold less active than wild-type enzyme (Parsonage *et al*., 2005). Since the A-type interface is most widespread among bacterial Prxs and because the A-type interface has some linkage to catalytic activity, Sarma *et al*. (2005) proposed that it is the more ancestral mode of association for Prxs.

6.2. Variations in the Presence and Placement of the Resolving Cys

The universal mechanism of Prxs (Figure 1) involves a single conserved peroxidatic Cys residue, but there is a diversity as to where the resolving Cys comes from. Prxs that do not contain a resolving Cys are called 1-Cys Prxs and for these enzymes the regeneration of the reduced C_P must be achieved by a different protein or small molecule reductant. Prxs that have a resolving Cys are called 2-Cys Prxs and are divided into two classes: "typical 2-Cys Prxs" are a narrow group with the resolving Cys coming from the other chain of a B-type dimer, and "atypical 2-Cys Prxs" are a broad grouping that includes all 2-Cys Prxs that are not "typical". Known atypical 2-Cys Prxs have the resolving Cys positioned in one of three distinct places: Prx5 Prxs have it in the loop between strand β7 and helix α5, Tpx Prxs have it in helix α3, and BCP Prxs have it in helix α2 just 5 residues beyond C_P. These

distinct placements of C_R imply that this family has an evolutionary history that involves multiple independent (convergent) conversions between 1-Cys and 2-Cys mechanisms, and that basically any place that can locally unfold to form a disulfide with C_P is a potential acceptable spot for C_R.

6.2.1. Subfamily Prx1: sensitive and robust varieties of typical 2-Cys Prxs

Prxs of the Prx1 subfamily form strong B-type dimers as their basic unit, stabilized by a C-terminal subdomain that associates strongly with the second domain of the dimer (Figure 6b). All enzymes assigned to this subfamily are typical 2-Cys Prxs with the C_R residue present in the C-terminal extension of the other chain of a B-type dimer. The C_R residue in these enzymes is buried within the folded C-terminal subdomain and is about 14 Å away from C_P in the fully-folded form (Figure 7a). Thus for resolution to occur in these enzymes, not only does the peroxidatic active site need to locally unfold to expose C_P, but the C-terminal subdomain must unfold to expose C_R. The result is that in the disulfide-bonded form of these enzymes the C-terminal extension becomes largely disordered and is generally not visible in the crystal structures (Figure 7a). In terms of the conformation of the locally unfolded C_P-loop, two variations have been seen, one that just involves unwinding of first turn of the helix (designated LU_{PRX1} in Figure 5) and a second that involves an additional shift in the direction of helix α2 (designated LU_{PRX1}' in Figure 5). As described by Wood *et al*. (2002), the structure of the dimeric *R. norvegicus* PrxI (Hirotsu *et al*., 1999) suggests that when the disulfide-bonded decamer dissociates into dimers, the C_P-loop undergoes a further conformational change to a more compact structure (designated LU_{PRX1}" in Table 1) that may enhance its ability to be recycled by thioredoxin or other reductant to regenerate the C_P and C_R thiols.

While all Prx1 subfamily enzymes share the above structural transitions, they can be subdivided into two distinct groups based on their sensitivity to the overoxidative inactivation shunt described earlier (Figure 1), which occurs when the active site S_POH reacts with a second molecule of peroxide. Certain types of these enzymes, such as human PrxI and PrxII are sensitive to such inactivation while others, such as the various bacterial AhpC enzymes, are robust (Wood *et al*., 2003b). The structural origin of this difference was discovered to be the presence in sensitive enzymes of a C-terminal helix that packed on top of the base of helix α2 and hindered the local unfolding of the peroxidatic active site (Figure 8). With reference to Figure 1, it can be seen that if local unfolding is an unfavorable event (i.e. K_{LU} is small), then flow down the overoxidation shunt will be enhanced making the enzyme more sensitive to oxidative inactivation. This structural explanation has been biochemically confirmed by protein engineering of two Prxs from *Schistosoma mansoni* (Sayed *et al*., 2004). To provide a rationale for why sensitivity to inactivation by peroxides has been selected for during evolution, Wood *et al*. (2003a) speculated that it allows these proteins to act as a peroxide floodgate to regulate hydrogen peroxide signaling in eukaryotes. This and other possible explanations are the subject of other Chapters in this volume.

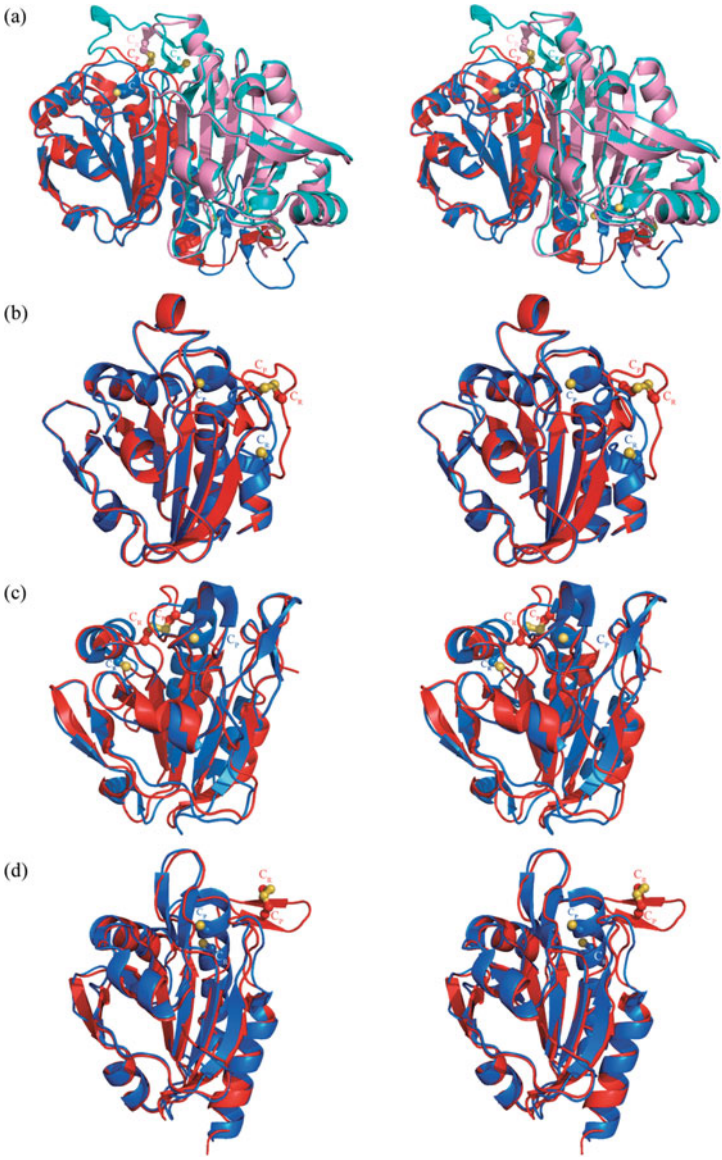

Figure 7. The local-unfolding conformational changes involved in resolution. Stereoviews are shown overlaying a representative fully-folded (blue tones) and locally-unfolded (red tones) structure from each of four Prx subfamilies: (a) the Prx1 subfamily represented by the B-type dimeric building block of *S. typhimurium* AhpC, with each chain of the dimer colored a distinct shade; (b) the Prx5 subfamily represented by human PrxV with an inferred locally-unfolded structure (see text); (c) the Tpx subfamily represented by *M. tuberculosis* and *H. influenzae* Tpx; (d) the BCP subfamily represented by *A. pernix* BCP. The C_P and C_R residues are shown as ball-and-stick models in each structure with S_P and S_R colored mustard yellow (See Plate 6)

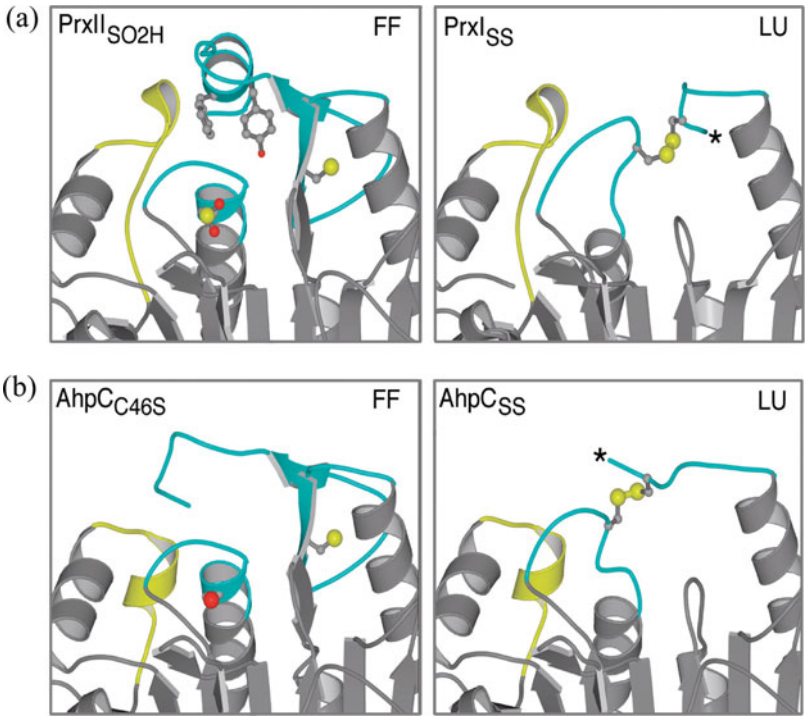

Figure 8. The structural difference between robust and sensitive typical 2-Cys Prxs. Views of (a) a sensitive Prx and (b) a robust Prx in the fully-folded forms (left panels) and in the locally-unfolded forms (right panels). In sensitive Prxs but not in robust Prxs, a C-terminal helix with a well conserved Tyr-Phe motif packs above the start of helix α2, and like a cork in a bottle stabilizes the fully-folded conformation, hindering its unfolding. This slows the resolution reaction and favors overoxidation by reaction with a second molecule of peroxide. In the locally-unfolded forms, an asterisk indicates the presence of additional disordered C-terminal residues. Figure reprinted from Wood *et al*. (2003a) *Science* **300**, 650–653 with permission (See Plate 7)

6.2.2. Subfamily Prx6

Subfamily Prx6 members studied thus far have a C-terminal extension that is even longer than the Prx1 enzymes, and include both 1-Cys and typical 2-Cys enzymes (Table 1). For the 1-Cys enzymes there is of course no resolving Cys required. The structurally known 2-Cys enzyme is representative of a group of archael Prxs having decameric structure and a C-terminally located C_R that would appear to be mechanistically indistinguishable from the typical 2-Cys enzymes in the Prx1 subfamily. However, these enzymes are distinct in that the C_R residue is positioned about 35 residues later in the sequence and is often present in close association with a third Cys in a CXDWWFC$_R$ motif (Mizohata *et al*., 2005). The third Cys is not essential but may facilitate catalysis in certain circumstances. In the folded protein C_R and C_P are 13 Å apart and while no structure of a disufide form is yet

known, as for Prx1 enzymes, disufide formation must require some disordering of the C-terminal extension as well as local unfolding of the C_P region.

6.2.3. Subfamily Prx5

The Prx5 subfamily also has both 1-Cys and 2-Cys (human Prx5) members, with 1-Cys members seemingly being more common (Copley *et al*., 2004). For human PrxV, the C_R residue is located in the turn between β7 and α5 and is 14 Å away from C_P (Figure 7b). No crystal structure is yet available for the catalytically relevant intramolecular disulfide form, but a structure for this form has been inferred from a fortuitous crystal structure of human Prx5 that includes an intermolecular disulfide between C_P of one dimer with C_R from another dimer (Evrard *et al*., 2004). This structure reveals that disulfide formation involves unfolding of the first half of helix α5 as well as the unfolding of the C_P-loop (Figure 7b).

6.2.4. Subfamily Tpx

The Tpx subfamily members all are atypical 2-Cys Prxs with the C_R residue coming from within the C-terminal portion of helix α3 (Figure 3). The first structure solved in this family was for the disulfide form of *E. coli* Tpx (Choi *et al*., 2003), and in this protein helix α3 (called α2 in that paper) was much shorter, and C_R was located in the middle of a fairly long and mobile loop. The authors proposed, based on comparisons with fully-folded Prx structures, that in the dithiol form of Tpx the C_R-containing chain segment would become helical and C_P and C_R would be separated by ∼13 Å (Choi *et al*., 2003). The unpublished structures now available for two fully-folded Tpxs (see Table 1) confirms those predictions (Figure 7c), revealing that resolution for this family requires the local unfolding of parts of both α2 and α3. During this structural change, a well-conserved aromatic residue just preceding C_R tucks into the protein core vacated by the first turn of α2 when it unfolds.

6.2.5. Subfamily BCP

The structurally known BCP subfamily members are all atypical 2-Cys Prxs with the C_R residue located just five residues beyond C_P (Figure 3). Apparently some BCP members are 1-Cys Prxs, as they do not have this Cys residue present (See Table 3.2 of Copley *et al*., 2004). Interestingly, in an unpublished structure of *A. pernix* BCP, a 2-Cys Prx having two dimers in the asymmetric unit has one chain from each dimer in the fully-folded conformation and one chain in the disulfide bonded locally-unfolded conformation. Based on this structure, in the fully-folded enzyme C_P and C_R are 12 Å apart on successive turns of the α2 helix, and resolution involves complete unraveling of the α2 helix and the formation of a short beta-hairpin with the strands bridged by the disulfide (Figure 7d). Whether the redox asymmetry observed in the crystal reflects an asymmetry in solution chemistry of the dimer is not known.

7. OUTLOOK

In terms of structural understanding, the eight years of work since the first Prx structure was solved have seen much exciting progress, so that a firm foundation of knowledge exists that will support biochemical and biomedical research of all types of Prxs. The major remaining hole in structural knowledge of Prxs comes from the complete lack of structures of wild-type and mutant enzymes in complex with known substrates, products, or inhibitors. This is an exciting area for future research that will expand our currently rather limited understanding of detailed structural aspects of substrate recognition and enzyme mechanism.

ACKNOWLEDGEMENTS

The authors thank Leslie Poole for editorial suggestions, and Kara Miles-Rockenfield for help with the preparation of figures. The authors' joint research program with Leslie Poole on peroxiredoxins is supported by National Institutes of Health grant RO1 GM050389.

REFERENCES

Alphey, M.S., Bond, C.S., Tetaud, E., Fairlamb, A.H., Hunter, W.N., 2000, The structure of reduced tryparedoxin peroxidase reveals a decamer and insight into reactivity of 2-Cys-peroxiredoxins. *J. Mol. Biol*. **300**: 903–916.

Berman, H.M., Westbrook, J., Feng, Z., Gilliland, G., Bhat, T.N., Weissig, H., Shindyalov, I.N., Bourne, P. E., 2000, The Protein Data Bank. *Nucleic Acids Res*. **28**: 235–242.

Biteau, B., Labarre, J.,Toledano, M.B., 2003, ATP-dependent reduction of cysteine-sulphinic acid by S. cerevisiae sulphiredoxin. *Nature* **425**: 980–984.

Bouillac, S., Rouhier, N., Tsan, P., Jacquot, J.P.,Lancelin, J.M., 2004, (1)H, (13)C and (15)N NMR assignment of the homodimeric poplar phloem type II peroxiredoxin. *J. Biomol. NMR* **30**: 105–106.

Bruns, C.M., Hubatsch, I., Ridderstrom, M., Mannervik, B., Tainer, J.A., 1999, Human glutathione transferase A4-4 crystal structures and mutagenesis reveal the basis of high catalytic efficiency with toxic lipid peroxidation products. *J. Mol. Biol*. **288**: 427–439.

Cao, Z., Roszak, A.W., Gourlay, L. J., Lindsay, J.G., Isaacs, N.W., 2005, Bovine mitochondrial peroxiredoxin III forms a two-ring catenane. *Structure (Camb.)* **13**: 1661–1664.

Chae, H.Z., Robison, K., Poole, L.B., Church, G., Storz, G., Rhee, S.G., 1994, Cloning and sequencing of thiol-specific antioxidant from mammalian brain: alkyl hydroperoxide reductase and thiol-specific antioxidant define a large family of antioxidant enzymes. *Pro.c Natl. Acad. Sci. USA* **91**: 7017–7021.

Chang, T.S., Jeong, W., Woo, H.A., Lee, S.M., Park, S., Rhee, S.G., 2004, Characterization of mammalian sulfiredoxin and its reactivation of hyperoxidized peroxiredoxin through reduction of cysteine sulfinic acid in the active site to cysteine. *J. Biol. Chem*. **279**: 50994–51001.

Chauhan, R., Mande, S.C., 2001, Characterization of the Mycobacterium tuberculosis H37Rv alkyl hydroperoxidase AhpC points to the importance of ionic interactions in oligomerization and activity. *Biochem. J*. **354**: 209–215.

Choi, H.J., Kang, S.W.,Yang, C.H., Rhee, S.G., Ryu, S.E.,1998, Crystal structure of a novel human peroxidase enzyme at 2.0 A resolution. *Nat. Struct. Biol*. **5**: 400–406.

Choi, J., Choi, S., Cha, M.K., Kim, I.H., Shin, W., 2003, Crystal structure of Escherichia coli thiol peroxidase in the oxidized state: insights into intramolecular disulfide formation and substrate binding in atypical 2-Cys peroxiredoxins. *J. Biol. Chem*. **278**: 49478–49486.

Choi, J., Choi, S., Chon, J.K., Cha, M.K., Kim, I.H., Shin, W., 2005, Crystal structure of the C107S/C112S mutant of yeast nuclear 2-Cys peroxiredoxin. *Proteins* **61**: 1146–1149.

Chothia, C., Lesk, A.M., 1986, The relation between the divergence of sequence and structure in proteins. *EMBO J.* **5**: 823–826.

Copley, S.D., Novak, W.R., Babbitt, P.C., 2004, Divergence of function in the thioredoxin fold suprafamily: evidence for evolution of peroxiredoxins from a thioredoxin-like ancestor. *Biochemistry* **43**: 13981–13995.

Declercq, J.-P., Evrard, C., Clippe, A., van der Stricht, D., Knoops, B., 2001, Crystal structure of human peroxiredoxin 5, a novel type of mammalian peroxiredoxin at 1.5 A resolution. *J. Mol. Biol.* **311**: 751–759.

Echalier, A., Trivelli, X., Corbier, C., Rouhier, N., Walker, O., Tsan, P., Jacquot, J.P., Aubry, A., Krimm, I., and Lancelin, J.M., 2005, Crystal structure and solution NMR dynamics of a D (type II) peroxiredoxin glutaredoxin and thioredoxin dependent: a new insight into the peroxiredoxin oligomerism. *Biochemistry* **44**: 1755–1767.

Evrard, C., Capron, A., Marchand, C., Clippe, A., Wattiez, R., Soumillion, P., Knoops B., and Declercq, J.P., 2004, Crystal structure of a dimeric oxidized form of human peroxiredoxin 5. *J. Mol. Biol.* **337**: 1079–1090.

Guimaraes, B.G., Souchon, H., Honore, N., Saint-Joanis, B., Brosch, R., Shepard, W., Cole, S.T., and Alzari, P.M., 2005, Structure and mechanism of the alkyl hydroperoxidase AhpC, a key element of the Mycobacterium tuberculosis defense system against oxidative stress. *J Biol. Chem.* **280**: 25735–25742.

Hirotsu, S., Abe, Y., Okada, K., Nagahara, N., Hori, H., Nishino T., and Hakoshima, T., 1999, Crystal structure of a multifunctional 2-Cys peroxiredoxin heme-binding protein 23 kDa/proliferation-associated gene product. *Proc. Natl. Acad. Sci. USA* **96**: 12333–12338.

Immenschuh, S., and Baumgart-Vogt, E., 2005, Peroxiredoxins, oxidative stress, and cell proliferation. *Antioxid. Redox Signal.* **7**: 768–777.

Kang, S.W., Rhee, S.G., Chang, T.S., Jeong W., and Choi, M.H., 2005, 2-Cys peroxiredoxin function in intracellular signal transduction: therapeutic implications. *Trends Mol. Med.* **11**: 571–578.

Kim, S.J., Woo, J.R., Hwang, Y.S., Jeong, D.G., Shin, D.H., Kim K., and Ryu, S.E., 2003, The tetrameric structure of Haemophilus influenza hybrid Prx5 reveals interactions between electron donor and acceptor proteins. *J. Biol. Chem.* **278**: 10790–10798.

Kitano, K., Niimura, Y., Nishiyama Y., and Miki, K.,1999, Stimulation of peroxidase activity by decamerization related to ionic strength: AhpC protein from Amphibacillus xylanus. *J. Biochem. (Tokyo)* **126**: 313–319.

Kristensen, P., Rasmussen D.E., and Kristensen, B.I., 1999, Properties of thiol-specific anti-oxidant protein or calpromotin in solution. *Biochem. Biophys. Res. Commun.* **262**: 127–131.

Li, S., Peterson, N.A., Kim, M.Y., Kim, C.Y., Hung, L.W., Yu, M., Lekin, T., Segelke, B.W., Lott J.S., and Baker, E.N., 2005, Crystal Structure of AhpE from Mycobacterium tuberculosis, a 1-Cys peroxiredoxin. *J. Mol. Biol.* **346**: 1035–1046.

Mizohata, E., Sakai, H., Fusatomi, E., Terada, T., Murayama, K., Shirouzu M., and Yokoyama, S., 2005, Crystal structure of an archaeal peroxiredoxin from the aerobic hyperthermophilic crenarchaeon Aeropyrum pernix K1. *J. Mol. Biol.* **354**: 317–329.

Nakamura, T., Yamamoto, T., Inoue, T., Matsumura, H., Kobayashi, A., Hagihara, Y., Uegaki, K., Ataka, M., Kai Y., and Ishikawa, K., 2006, Crystal structure of thioredoxin peroxidase from aerobic hyperthermophilic archaeon *Aeropyrum pernix* K1. *Proteins* **62**: 822–826.

Papinutto, E., Windle, H.J., Cendron, L., Battistutta, R., Kelleher D., and Zanotti, G., 2005, Crystal structure of alkyl hydroperoxide-reductase (AhpC) from Helicobacter pylori. *Biochim. Biophys. Acta* **1753**: 240–246.

Parsonage, D., D. S. Youngblood, G. N. Sarma, Z. A. Wood, P. A. Karplus and L. B. Poole, 2005, Analysis of the link between enzymatic activity and oligomeric state in AhpC, a bacterial peroxiredoxin. *Biochemistry* **44**: 10583–10592.

Pineyro, M.D., Pizarro, J.C., Lema, F., Pritsch, O., Cayota, A., Bentley G.A., and Robello, C., 2005, Crystal structure of the tryparedoxin peroxidase from the human parasite Trypanosoma cruzi. *J. Struct. Biol.* **150**: 11–22.

Sarma, G.N., Nickel, C., Rahlfs, S., Fischer, M., Becker K., and Karplus, P.A., 2005, Crystal structure of a novel Plasmodium falciparum 1-Cys peroxiredoxin. *J. Mol. Biol*. **346**: 1021–1034.

Sayed, A.A., and Williams, D.L., 2004, Biochemical characterization of 2-Cys peroxiredoxins from Schistosoma mansoni. *J. Biol. Chem*. **279**: 26159–26166.

Schröder, E., Littlechild, J.A., Lebedev, A.A., Errington, N., Vagin A.A., and Isupov, M.N., 2000, Crystal structure of decameric 2-Cys peroxiredoxin from human erythrocytes at 1.7 A resolution. *Structure Fold. Des*. **8**: 605–615.

Schröder, E., Willis A.C., and Ponting, C.P., 1998, Porcine natural-killer-enhancing factor-B: oligomerisation and identification as a calpain substrate in vitro. *Biochim. Biophy. Acta* **1383**: 279–291.

Stehr, M., Hecht, H.-J., Jäger, T., Flohé, L., and Singh, M.,2006, Structure of the inactive variant C60S of *Mycobacterium tuberculosis* thiol peroxidase. *Acta Crystallogr. D. Biol. Crystallogr*. **62**: 563–567.

Trivelli, X., Krimm, I., Ebel, C., Verdoucq, L., Prouzet-Mauleon, V., Chartier, Y., Tsan, P., Lauquin, G., Meyer Y., and Lancelin, J.M., 2003, Characterization of the yeast peroxiredoxin Ahp1 in its reduced active and overoxidized inactive forms using NMR. *Biochemistry* **42**: 14139–14149.

Woo, H.A., Chae, H.Z., Hwang, S.C., Yang, K.S., Kang, S.W., Kim K., and Rhee, S.G., 2003, Reversing the inactivation of peroxiredoxins caused by cysteine sulfinic acid formation. *Science* **300**: 653–656.

Wood, Z. A., Poole, L.B., Hantgan R.R., and Karplus, P.A., 2002, Dimers to doughnuts: redox-sensitive oligomerization of 2-cysteine peroxiredoxins. *Biochemistry* **41**: 5493–5504.

Wood, Z.A., Poole L.B., and Karplus, P.A., 2003a, Peroxiredoxin evolution and the regulation of hydrogen peroxide signaling. *Science* **300**: 650–653.

Wood, Z.A., Schröder, E., Harris J.R., and Poole, L.B., 2003b, Structure, mechanism and regulation of peroxiredoxins. *Trends Biochem. Sci*. **28**: 32–40.